Thermoplastic Induction Welded Joint Design for Structural Health Monitoring Damage Detectability

MATTIA MAZZESCHI[1], ADRIAN PEDROSA VALBUENA[1], KARINA CARLA NUNEZ[1,2], MAITE FERNANDEZ[1], ESTEBAN CANIBANO[1,3] and JUAN CARLOS MERINO[1,2]

ABSTRACT

In the present work, the design of thermoplastic induced welded joints was carried out considering different aspects related to structural performance, manufacturability and structural health monitoring capability. Three lap-joints configurations were considered: two of them having welded plates with two different carbon fibers plies stacked layups and one obtained by welding carbon fibers fabric laminates. A numerical analysis was carried out by performing (i) structural simulations to assess the mechanical properties of the joints, (ii) induction welding process simulations to evaluate temperature distribution in the welded interface area and (iii) damage detection assessment by reproducing the response of a structural health monitoring sensor bonded in correspondence of the joint overlap area. Electromagnetic-based structural health monitoring techniques were employed to evaluate local variation of electromagnetic characteristics due to defect presence. The results obtained show that the design choices have a significant influence on the physical properties of the welded material such as the electrical conductivity anisotropy. The different induced currents distribution obtained during both the fabrication and damage inspection phase, affects respectively the manufacturing and detection capability.

An experimental validation was carried out by mechanical tests under quasi-static loading for the case with the best tradeoff between structural performance, manufacturing feasibility and damage detection capability. The proposed approach show the importance of taking into account the requirement of damage detectability from an early stage of the design.

[1]Mattia Mazzeschi, Adrian Pedrosa Valbuena, Karina Carla Nuñez, Maite Fernandez, Esteban Cañibano, Juan Carlos Merino, Cidaut Foundation, Parque Tecnológico de Boecillo, 47151 Boecillo, Spain

[2]Karina Carla Nuñez, Juan Carlos Merino, Department of Condensed Matter Physics, Cristallography and Mineralogy, University of Valladolid, Industrial Engineering, 47011 Valladolid, Spain

[3]Esteban Cañibano, Department of Industrial Engineering, University of Valladolid, 47011 Valladolid, Spain

INTRODUCTION

Thermoplastic welding contributes to the cost-effectiveness in manufacturing of thermoplastic composites overcoming numerous issues associated with conventional joining processes such as extensive surface preparation and long curing cycles that characterizes adhesive bonding processes or stress concentration and intense labor typical of mechanical fastening. Among the various techniques, ultrasonic [1], resistance[2] and induction welding [3] are considered to be most suitable for thermoplastics. Induction welding potentially allows for geometrically complex welds and does not oblige any contact with the welding stack for heating, which increases flexibility and simplifies automation [4]. Generally, the typical approach in the design of a structural joint is to ensure primarily a certain structural performance. Moreover, the concurring engineer's approach tries to simultaneously ensure other targets such as manufacturability and maintainability. Thanks to recent developments in the field of structural health monitoring and the potential benefits it could bring, robust damage detectability and residual life estimation are additional requirements having an increasing importance also during the design phase. The physical and mechanical properties that characterize a selected material have an influence on the damage sensing capability for a given SHM technology.

The aim of this work is to evaluate how the physical and mechanical properties of CF/PAEK laminates influence the structural performance, the viability of the thermoplastic induction welding process and the damage sensitivity for a given SHM method.

Electromagnetic-based SHM techniques are relatively uninvestigated for not perfectly conductive material [5]–[7] and are currently the authors' main research focus. The present analysis is limited to electromagnetic-based SHM techniques but it could be potentially be carried out again with different SHM techniques. In both the thermoplastic induction welding process and the quality inspection of the joint using electromagnetic based SHM techniques, the material electrical conductivity is most relevant property in terms of manufacturing and inspection performance. In fact, the local values of the electrical conductivity affect the eddy currents distribution induced in the material during the induction welding process and therefore the amount of energy dissipated in terms of heat. Moreover, damage presence affects locally the electromagnetic characteristics of the material. The difference in conductivity and the distribution of eddy currents between the sound and defective condition determines the level of sensitivity for a given electromagnetic-based sensor. For these reasons, electrical conductivity was the main property examined in this study in order to compare the weldability and damage detection capability for different CF/PAEK laminates configurations. In addition, the mechanical properties of the considered joints were also evaluated to compare the structural performances.

METHODOLOGY

Numerical Methods

MATERIAL PROPERTIES

Three different CF/PAEK lap-joints were considered varying the type of adherents to be welded: two different laminates configurations having stacking sequence (*i*) $[(0,30,60,90)]_{symm}$ and (*ii*) $[(0,45,70,90)]_{symm}$ respectively and (*iii*) 5HS woven fabric-reinforced laminates. The same thickness of the CF/PAEK plates of 2.48 mm was assumed for each type of union. The electrical, thermal and mechanical properties have been defined to correctly simulate the physics of the different simulations. *TABLE I* reassumes the main properties used in FEM simulations.

DAMAGE SENSING AND INDUCTION WELDING MODELLING

Figure 2.a shows the constitutive elements of the electromagnetic-based sensor, designed as a result of a previous autor's work[6] and employed in the present study as SHM sensing techniques. A magnetic field generated by a sinusoidal time variant current flowing in an emission loop, interacts with the underlying material being inspected. The local measurement of the resulting magnetic field is performed by a reception loop placed concentrically and below the emission loop.

The damage sensing performances were evaluated comparing the frequency response between 0.1 and 4 MHz of a sound and defective welded joint for all three joint configuration. The AC/DC module of the software COMSOL® Multiphysics was used to model the frequency response of EM sensors placed in correspondence of the joint overlap area (Figure 2.b). In order to reproduce the presence of a lack of weld or a loss of joint surface area, a 0.1 mm thick and 8x8 mm in size layer placed in the bond line was modelled assuming the same value of the conductivity of the air (Figure 2.b).

The simulation of the induction welding process was also conducted using AC/DC module of the software COMSOL® Multiphysics but coupled with heat transfer (HT) module (Figure 2.c). During the subroutine calculation, electromagnetism equations were solved for the prediction of the eddy currents distribution in joints plates.

TABLE I MATERIAL PROPERTIES USED IN THE FEM (DATA ESTIMATED FROM [8]–[13].

Material properties		**Laminates configuration**		
		$[(0,30,60,90)]_{symm}$	**$[(0,45,70,90)]_{symm}$**	**5HS woven fabric**
Electrical	Electrical conductivity at 22ºC* [S/m]	σ_x=11300, σ_y =105, σ_z=44	σ_x=11300, σ_y =105, σ_z=44	σ_x=11300, σ_y =11300, σ_z=44
	Magnetic permeability	μ_r=1	μ_r=1	μ_r=1
Thermal	Specific heat at 22ºC* [J/(kgºC)]	920	920	920
	Thermal conductivity [W/(mK)]	k_x=2.22, k_y=0.33 5, k_z=0.335	k_x=2.22, k_y=0.3 35, k_z=0.335	k_x=2.22, k_y=2.2 2, k_z=0.335
Mechanical	Tensile modulus, [MPa]	E_{xx}=135000, E_{yy}=10000, E_{zz}=1 0000	E_{xx}=135000, E_{yy}=10000, E_{zz} =10000	E_{xx}=58000, E_{yy}=59000, E_{zz} =3900
	Tensile stress [MPa]	S_{xx}=2410, S_{yy}=86 , S_{zz}=86	S_{xx}=2410, S_{yy}= 86, S_{zz}=86	S_{xx}=805, S_{yy}=7 39, S_{zz}=159
	Poisson's ratio	ν_{12}=0.35,ν_{23}=0.07 5,ν_{31}=0.075	ν_{12}=0.35,ν_{23}=0. 075,ν_{31}=0.075	ν_{12}=0.35,ν_{23}=0. 075,ν_{31}=0.075

*For temperature-dependent properties see *Figure 1*.

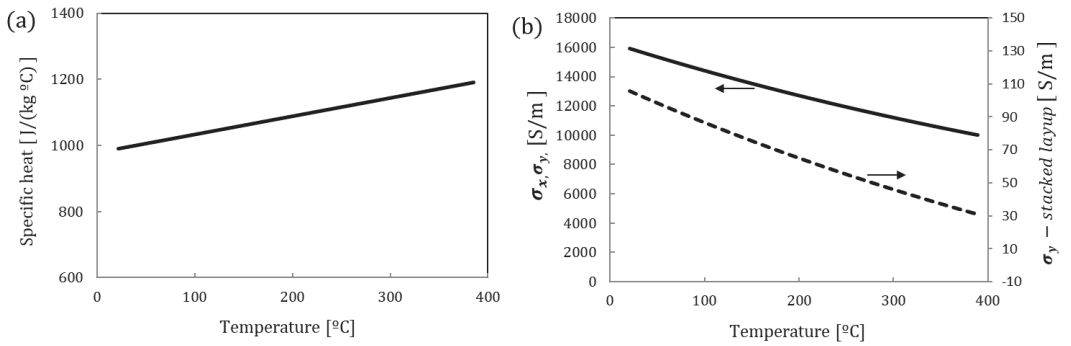

Figure 1 (a) Specific heat and (b) electrical conductivity as a function of temperature.

A transient HT thermal analysis then served to calculate the heat generated by the eddy currents (Joule effect) as well the temperature distribution taking into account conduction, convection, and radiation HT mechanisms. The different temperature-dependent properties of the materials are redefined when the temperature changes exceed a certain threshold and the calculation is subsequently updated until the desired heating time is reached.

The assumption taken in the model were the following: (*i*) the thermal expansion of materials is neglected, (*ii*) convection coefficient of h=5 W/(m^{2}K) is considered based on [11] (*iii*) Joule losses are the only heating mechanism and dielectric and junction heating are neglected. The three different joint configurations were compared by evaluating the temperature distribution in the welded interface for a given heating time.

LAP SHEAR TEST MODELLING

Commercially available FE software MSC Marc/Mentat was used to reproduce lap-shear tests and compare the stress field in the welded interface for the three different considered joint materials. Mesh was generated using Altair Hypermesh. The geometry of the specimens was established according to ASTM D1002, modelling 25.4 x 101.6 mm^2 upper and lower plates with a nominal overlap of 13.8 mm. In order to reproduce the welded zone, the "glued contact" feature was imposed for the nodes in common between lower and upper plate and the properties of the PAEK thermoplastic matrix was assigned to the adjacent tetrahedral elements. The properties of the thermoplastic matrix were as shown in *TABLE II*.

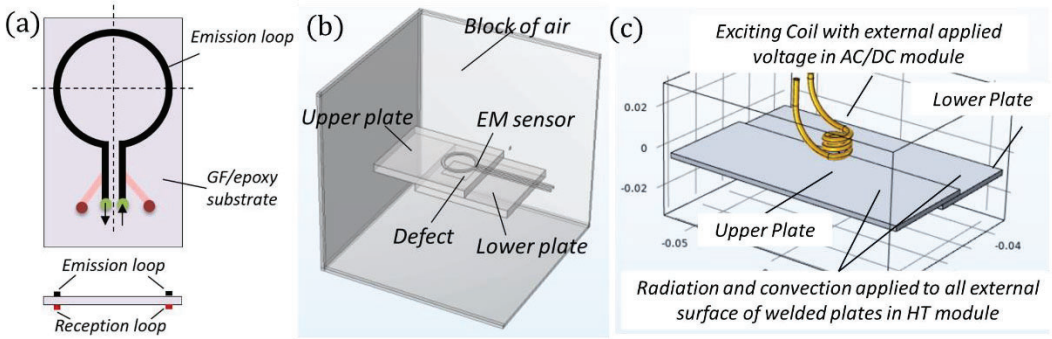

Figure 2 (a) EM sensor constitutive elements. (b) Model employed in damage sensing simulations. (c) FEM geometry of induction welding model.

TABLE II MECHANICAL PROPERTIES EMPLOYED FOR MODELLING THE CONSOLIDATED MATRIX (PAEK) IN THE WELDED AREA.

Tensile modulus [MPa]	Tensile Stress [MPa]	Poisson's ratio
3200	87.0	0.42

RESULT AND DISCUSSION

Numerical results

In the majority of SHM application, changes of a reference signal corresponding to the sound structure are of special interest to detect damage that induces a local variation of a specific property of the material. The following parameter is considered in order to evaluate the sensitivity (ΔV) to a damage:

$$\Delta V = 20log_{10}\left[\frac{V_{defect}}{V_{sound}}\right] \quad (1)$$

where V_{defect} and V_{sound} are, respectively, the induced voltage ofthe reception coil in the presence and absence of a defect. Figure 3 shows the EM sensor damage sensitivity where it is possible to appreciate frequency response changes depending on the CF thermoplastic composites that constitute the joints. It is possible to identify a peak of maximum sensitivity around 2 MHz when inspecting joints with 5HS woven fabric laminates. In contrast for thermoplatic welded joint whose adherents are stacked laminates, the damage sensitivity shows a continuous increasing trend with frequency for both stacking sequences. At equal frequency EM sensors show a greater ability to identify a given damage when the welded laminates have a [0,45,70,90]s stacking sequence rather than [0,30,60,90]s. However, in the frequency range considered EM sensor shows the highest sensitivity value in the presence of 5HS woven fabric laminates.

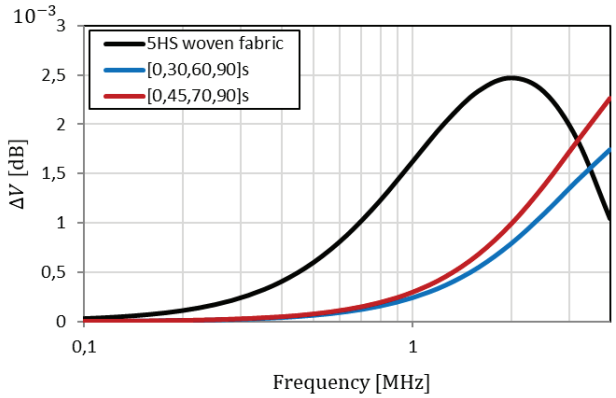

Figure 3 Damage sensitivity of EM sensor inspecting the three different welded CF thermoplastic composites.

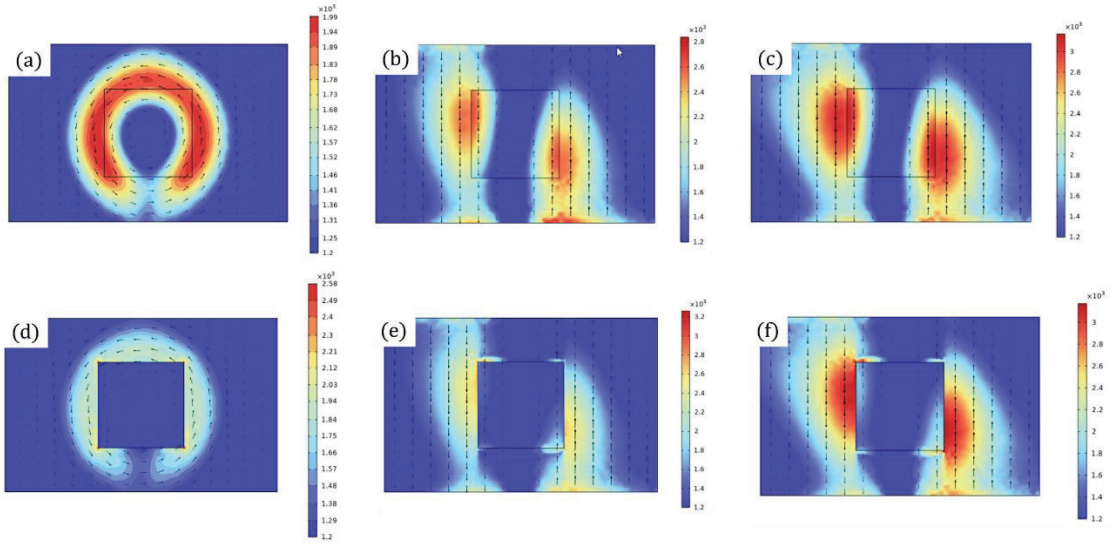

Figure 4 Intensity and distribution of current density on the welded interface for (a-c) sound and (d-f) defective joint when the CF thermoplastic materials of the adherents are (a, d) 5HS woven fabric laminates (at 1.99 MHz)., (b, e) unidirectional CF laminates with stacking sequence [0,30,60,90]s (at 3.98 MHz) and (c, f) [0,45,70, 90]s (at 3.98 MHz).

The different trends in damage sensitivity are explained by considering the different anisotropy of the electrical conductivity of the adherents that gives rise to a different distribution of induced currents. The different intensity and orientation with respect to the defect of the currents produces changes in the magnetic field measured by the EM sensor of different entity when moving from the sound to defective joint condition. Figure 4 shows the intensity and trajectory of the induced currents for the three cases considered in the absence and presence of a loss of welded area. Considering the homogenous electrical conductivity of 5HS woven fabric laminates in the plane, the induced currents tend to distribute with circular path in the case of sound structure (Figure 4.a). A different result is obtained for stacked laminates where the currents distribute parallel to the longitudinal direction of the CF fibers which is characterized by higher values of conductivity (Figure 4.b and c).

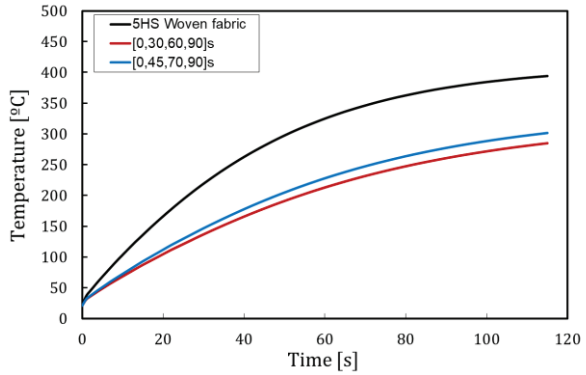

Figure 5 Temperature change over time in a point located in the welded area just below the inductive coil.

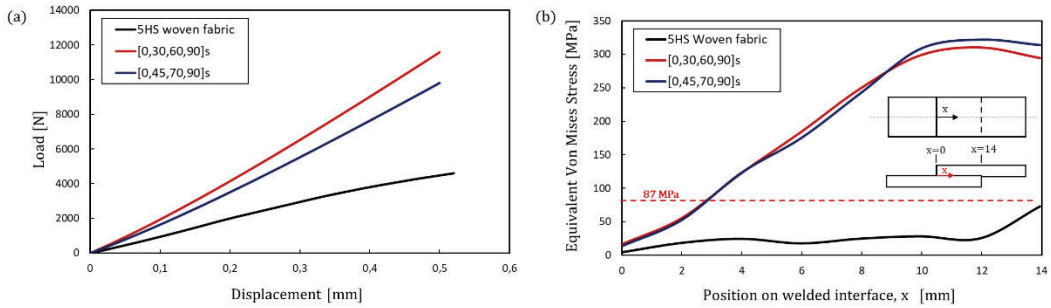

Figure 6 (a) Load-displacements curves and (b) stress distribution along the welded interface zone highlighting the PAEK tensile yield stress (displacement 0.25 mm).

Looking at Figure 4.d, the presence of a defect (modeled as a zone of almost zero conductivity) greatly reduces the of currents in the bondline, which produce a variation of current density maximum value of $0.59x10^3$ A/m^2. In the case of stacked laminates, on the other hand, the defect is found at zones of low current density and its presence does not greatly influence the distribution of induced currents. The greater extent of high-intensity zones for laminates whose stacking sequence is [0,45,70,90]s compared with [0,30,60,90]s justifies the higher damage sensitivity of the EM sensor observed in Figure 3.

The different distribution of induced currents in the considered materials also has an impact on processability during thermoplastic induction welding operations. Figure 5 shows the different inductive heating of the welded interface when a power of 2.9 kW is delivered from the exciting coil (see Figure 2.c) in the three cases considered. Higher temperature values are obtained for 5HS woven fabric laminates reaching a temperature of 389 ºC that is optimal for PAEK matrix processing. Significant lower temperatures are instead reached for stacked laminates, for which it would be necessary to increase the power of the inductive coil in order to make welding possible.

Slightly higher temperatures are noted for the [0,45,70,90]s configuration due to the higher intensity of the induced currents responsible of joule effect mechanism as already seen in the analysis of the damage sensitive results.

Finally, performing structural simulations allowed the mechanical performance of the three considered joints to be compared. Figure 6.a shows the load-displacement curves obtained by fixing one end of the joint and imposing a given displacement.

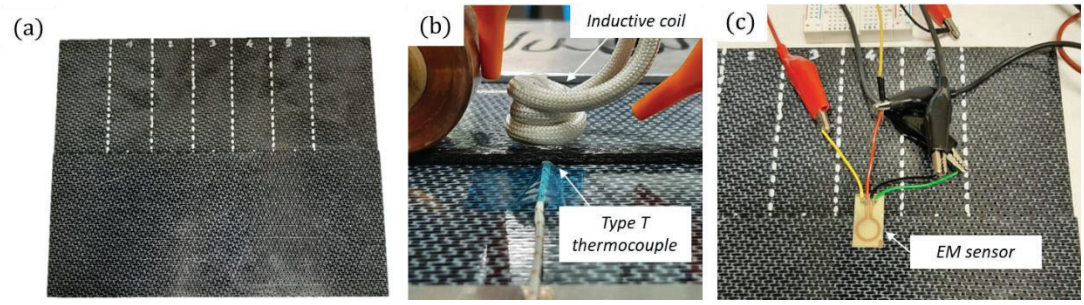

Figure 7 (a) Welded sample with marked areas where specimens were extracted for lap-shear tests. (b) Relative position between thermocouple and inductive coil. (c) EM sensor bonded in the overlap zone to obtain the frequency response of the reception loop.

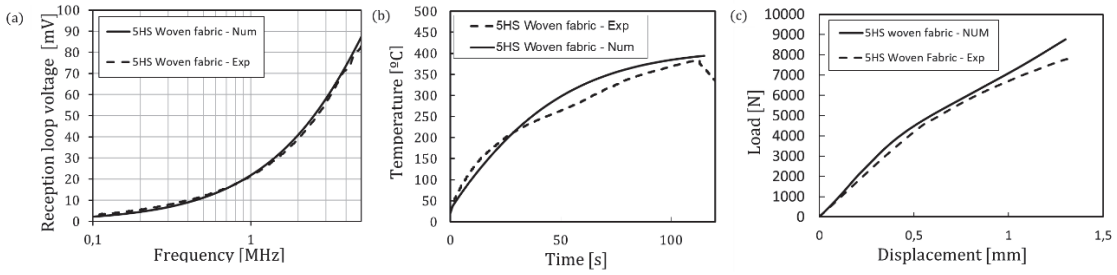

Figure 8 Numerical vs experimental data for (a) damage sensing, (b) induction welding and (c) structural FE models.

It shows that joined stacked laminates offer greater stiffness than 5HS woven fabric ones. However, looking at the stress distribution in the welded interface (Figure 6.b), joints with 5HS woven fabric show a more uniform stress distribution for a given displacement with stresses below the plasticization limit. This greater homogeneity of stresses in the bondline may potentially provide better fatigue properties, aspect not considered in the present study.

Experimental validation

In order to validate the models employed in the present study, welded specimen were manufactured employing 5HS woven fabric laminates considered the best tradeoff material with regard to damage sensing, weldability and mechanical performances.

A commercial induction welding machine (Bielec S.L.) was used to manufacture the welded specimen from which specimens were extracted for static test performed according to ASTM D1002 (Figure 7.a).

In one of the sample, a type T thermocouple was placed in the welded interface in order to have temperature data available for inductive welding model calibration (Figure 7.b). EM sensor was placed on the weld overlap zone in order to inspect the welds integrity and measure the voltage of the reception loop between 0.1 and 5 MHz (Figure 7.c). Figure 8 shows that for each model used, sufficient correlation between numerical and experimental data was obtained.

CONCLUSIONS

Based on the results just presented, the electrical properties of joints with 5HS fabric laminates allow EM sensor to have better damage sensitivity for the type of defect considered and better heating capability than joint configurations with stacked laminates. Although this type of joint offers lower stiffness the tensional state on the bondline appears more homogeneous than laminates with stacking sequences [0,45,70,90]s and [0,30,60,90]s. The present study has shown how the anisotropy of electrical properties has a significant impact not only in the viability of thermoplastic induction welding process but also in the performance of the considered electromagnetic based SHM technique.

REFERENCES

1. Y. Wang, Z. Rao, S. Liao, and F. Wang, “Ultrasonic welding of fiber reinforced thermoplastic composites: Current understanding and challenges,” Composites Part A: Applied Science and Manufacturing, vol. 149. Elsevier Ltd, 2021, doi: 10.1016/j.compositesa.2021.106578.
2. X. Xiong et al., “Resistance welding technology of fiber reinforced polymer composites: a review,” Journal of Adhesion Science and Technology, vol. 35, no. 15. Taylor and Francis Ltd., pp. 1593–1619, 2021, doi: 10.1080/01694243.2020.1856514.
3. S. Becker, M. Michel, P. Mitschang, and M. Duhovic, “Influence of polymer matrix on the induction heating behavior of CFRPC laminates,” Compos. Part B Eng., vol. 231, 2022, doi: 10.1016/j.compositesb.2021.109561.
4. L. Moser, P. Mitschang, and A. Schlarb, “Robot based induction welding of thermoplastic polymer composites,” Int. SAMPE Symp. Exhib., vol. 52, Jan. 2008.
5. M. B. Lemistre and D. L. Balageas, “A hybrid electromagnetic acousto-ultrasonic method for SHM of carbon/epoxy structures,” Struct. Heal. Monit., vol. 2, no. 2, pp. 153–160, 2003, doi: 10.1177/1475921703002002007.
6. M. Mazzeschi, K. C. Nuñez, E. Cañibano, and J. C. Merino, “Monitoring of thermoplastic induction welding defects. Use of electromagnetic properties as a predictive tool,” Struct. Heal. Monit., vol. 0, no. 2, pp. 1–15, 2022, doi: 10.1177/14759217221111979.
7. Q. Liu, H. Sun, T. Wang, and X. Qing, “On-site health monitoring of composite bolted joint using built-in distributed eddy current sensor network,” Materials (Basel)., vol. 12, no. 7, 2019, doi: 10.3390/ma12172785.
8. N. Athanasopoulos and V. Kostopoulos, “Prediction and experimental validation of the electrical conductivity of dry carbon fiber unidirectional layers,” Compos. Part B Eng., vol. 42, no. 6, pp. 1578–1587, 2011, doi: 10.1016/j.compositesb.2011.04.008.
9. Y. Guo, L. Shi, Z. Huang, and S. Fu, “Research on conductivity temperature dependence of CFRP,” IEEE Int. Symp. Electromagn. Compat., vol. 2017-Octob, no. October 2017, pp. 1–3, 2018, doi: 10.1109/EMC-B.2017.8260383.
10. P. D. Sheet and P. Type, “Toray Cetex TC1225 Toray Cetex TC1225,” vol. 31, no. 0, pp. 1–7.
11. P. Gouin O’Shaughnessey, M. Dubé, and I. Fernandez Villegas, “Modeling and experimental investigation of induction welding of thermoplastic composites and comparison with other welding processes,” J. Compos. Mater., vol. 50, no. 21, pp. 2895–2910, 2016, doi: 10.1177/0021998315614991.
12. M. Holland, M. J. L. van Tooren, D. Barazanchy, and J. Pandher, “Modeling of induction heating of thermoplastic composites,” J. Thermoplast. Compos. Mater., vol. 35, no. 10, pp. 1772–1789, 2022, doi: 10.1177/0892705720911979.
13. Sioutis and K. Tserpes, “A mixed-mode fatigue crack growth model for co-consolidated thermoplastic joints,” Int. J. Fatigue, vol. 173, no. March, p. 107682, 2023, doi: 10.1016/j.ijfatigue.2023.107682.